

Article

# Diffusion-Slip Boundary Conditions for Isothermal Flows in Micro- and Nano-Channels

Alwin Michael Tomy \*  and S. Kokou Dadzie 

School of Engineering and Physical Sciences, Heriot-Watt University, Edinburgh EH11 4AS, UK

\* Correspondence: amt4@hw.ac.uk

**Abstract:** Continuum description of flows in micro- and nano-systems requires ad hoc addition of effects such as slip at walls, surface diffusion, Knudsen diffusion and others. While all these effects are derived from various phenomenological formulations, a sound theoretical ground unifying these effects and observations is still lacking. In this paper, adopting the definition and existence of various type of flow velocities beyond that of the standard mass velocity, we suggest derivation of model boundary conditions that may systematically justify various diffusion process occurring in micro- and nano-flows where the classical continuum model breaks down. Using these boundary conditions in conjunction with the classical continuum flow equations we present a unified derivation of various expressions of mass flow rates and flow profiles in micro- and nano-channels that fit experimental data and provide new insights into these flow profiles. The methodology is consistent with recasting the Navier–Stokes equations and appears justified for both gas and liquid flows. We conclude that these diffusion type of boundary conditions may be more appropriate to use in simulating flows in micro- and nano-systems and may also be adapted as boundary condition models in other interfacial flow modelling.

**Keywords:** diffusion slip; volume diffusion; micro- and nano-channels



**Citation:** Tomy, A.W.; Dadzie, S.K. Diffusion-Slip Boundary Conditions for Isothermal Flows in Micro- and Nano-Channels. *Micromachines* **2022**, *13*, 1425. <https://doi.org/10.3390/mi13091425>

Academic Editors: Ridong Wang and Zhihua Pu

Received: 26 July 2022

Accepted: 26 August 2022

Published: 29 August 2022

**Publisher's Note:** MDPI stays neutral with regard to jurisdictional claims in published maps and institutional affiliations.



**Copyright:** © 2022 by the authors. Licensee MDPI, Basel, Switzerland. This article is an open access article distributed under the terms and conditions of the Creative Commons Attribution (CC BY) license (<https://creativecommons.org/licenses/by/4.0/>).

## 1. Introduction

Advancements in fabrication methods and developments in microfluidics are driving the research interests to understand the unconventional physics that govern the operation and manufacturing of micro- and nano- scale devices such as micropumps, heat exchangers for electronic devices, gas chromatography analyzers and other micro-electro-mechanical-systems [1–5]. Classical flow models such as the Navier–Stokes (N-S) equations with no-slip boundary condition are unable to replicate some of the phenomena pertaining fluid flows in the micro- and nano- length scales [6]. Experimentally, it has been observed and confirmed that there is a significant enhancement of fluid flow through micro- and nano- channels but classical continuum models fail to accurately predict the observed flow enhancement as well as other flow profiles such as non-linear pressure profiles [7–9]. Initial observations were made by Knudsen while investigating rarefied gas flows through narrow tubes [10]. Since then several studies have verified this enhancement for gas flows through micro-channels at various states of rarefaction [11–13] and for liquid flows through nano-tubes [7,8,14,15]. The degree of rarefaction in a gas is defined by its Knudsen number,  $Kn$ , as the ratio between the mean free path ( $\lambda$ ) of the gas particles to a characteristic length of the flowing system [16]. Based on the Knudsen number, gas flows are generally divided into four regimes: the continuum flow regime with  $Kn \leq 0.001$ , the slip flow regime with  $0.001 \leq Kn \leq 0.1$ , the transition regime with  $0.1 \leq Kn \leq 10$ , and the free molecular regime with  $Kn \geq 10$ . In an effort to extend the application of continuum flow models to predict non-conventional fluid flow phenomena in the rarefied regime, many researchers have over the years formulated slip boundary conditions and new continuum models e.g. Extended Navier–Stokes equations (ENSE) [17,18], Bi-velocity model [19] and Recast

Navier–Stokes (RNS) equations [20,21]. Of the velocity boundary conditions developed, the most elegant and widely used is the Maxwell slip model, introduced by James Clerk Maxwell in 1879 [22]. Arkilic et al. [11] analytically solved a simplified set of Navier–Stokes equations along with first-order Maxwell slip boundary conditions for micro-channel flow and successfully predicted the mass flow rate up to  $Kn \sim 0.1$ . For high values of Knudsen number, up to  $Kn \sim 1.2$ , the validity of N-S equations to predict these flow rates is seen to be improved by using a second-order slip boundary conditions with an appropriate selection of slip coefficients extracted from the given experimental data [23,24]. Karniadakis and Beskok [1] proposed a general slip boundary conditions, and their solution of N-S equations for a micro-channel case agrees well up to  $Kn = 5$ .

The concept of a diffusive velocity or a diffusive flux based on Fick's law has given rise to diffusive slip boundary condition and new continuum models such as ENSE, Bi-velocity model and Recast Navier–Stokes model. Adachi et al. [25] introduced a diffusion based velocity-slip boundary condition that is based on physical insights to predict the diffusive velocity at the wall. Veltzke and Thöming [26] have shown that a superposition of convective transport and Fickian diffusion term matches experimental data for micro-channel flows, up to Knudsen number of 0.4. Dongari et al. [27] provided analytical solution for the ENSE model applied for a micro-channel flow and validated the solutions against Direct Simulation Monte Carlo (DSMC) solutions, showing a good agreement in the early and late transition regimes ( $Kn < 0.3$  and  $1 < Kn < 10$ ). Brenner introduced the concept of volume diffusion hydrodynamics [6,28,29]. Dadzie and Brenner [30], on the basis of the volume diffusion hydrodynamics, derived analytical solution to micro-channel flows that agreed well with Ewart et al.'s [13] data up to Knudsen number of 5.

Motivated by the previous works, in this paper we provide a formulation of new velocity boundary conditions unifying the existing Maxwellian and diffusion velocities from recast Navier–Stokes models [20]. This new boundary conditions when used with the conventional Navier–Stokes equations, predict gas mass flow rates from the continuum to free-molecular regime. Additional terms appearing in the expressions for the flow rates directly link to the definition of the new diffusion velocities. The new boundary conditions also reveal new insights into the velocity and pressure profiles that are more consistent with the flow enhancement observed. For example, in the high Knudsen number regime, the flow profiles become clearly that of plug flows corroborating the high flow enhancement phenomena beyond the simple traditional wall slip velocity explanation.

The rest of the paper is organised as follows: In Section 2, we introduce the new diffusion-slip boundary conditions and the reduced governing equations for flows in micro-channels. Analytical solutions for micro- and nano-channel gas flows are derived in Section 2.4 and include effects of rarefaction as described in Section 2.3. In Section 3, we compare the dimensionless flow-rate predicted by the new model with experimental data and also present the solutions for velocity and pressure profiles at various states of rarefaction. Finally, in Section 4, we outline our concluding remarks based on the results of the study.

## 2. Governing Equations and the New Models

The present governing equations and models are based on the observation that a change in velocity variable in classical Navier–Stokes equations leads to various type of mass and volume diffusion continuum models [20].

### 2.1. Governing Equations

We consider the compressible Navier–Stokes set of equations to model flow through the micro-channels. In the absence of any temperature gradients the Navier–Stokes system of equations, ignoring the body force, for single species can be written in Cartesian coordinates as:

$$\frac{\partial \rho}{\partial t} + \frac{\partial(\rho U_i)}{\partial x_i} = 0, \tag{1}$$

$$\rho \left( \frac{\partial U_j}{\partial t} + U_i \frac{\partial U_j}{\partial x_i} \right) = - \frac{\partial P}{\partial x_j} - \frac{\partial \tau_{ij}}{\partial x_i}, \tag{2}$$

where  $i$  and  $j$  are the coordinate indices and  $\rho$ ,  $U$ ,  $P$  and  $\tau$  are the density, velocity, pressure and viscous stress, respectively. For a newtonian fluid,

$$\tau_{ij} = -\mu \left( \frac{\partial U_j}{\partial x_i} + \frac{\partial U_i}{\partial x_j} \right) + \frac{2}{3} \mu \delta_{ij} \frac{\partial U_k}{\partial x_k}, \tag{3}$$

where  $\mu$  is the dynamic viscosity and  $\delta_{ij}$  is the Kronecker Delta function, and equation of state for an ideal gas is given by,

$$P = \rho \mathcal{R} T, \tag{4}$$

where  $\mathcal{R}$  is the specific gas constant and  $T$  is the temperature. In this paper we consider an isothermal pressure driven flow of an ideal gas through a rectangular micro-channel of length  $L$ , width  $w$  and height  $h$ , as shown in Figure 1. The stream-wise coordinate is  $x$  with velocity  $U_x = u$ , the wall-normal coordinate is  $y$  with velocity  $U_y = v$ , and the height to length ratio is  $\epsilon = h/L$ . For the case of  $\epsilon \ll 1$  and  $h/w \ll 1$  we can consider the flow to be two-dimensional, neglecting the variations in the  $z$  direction.

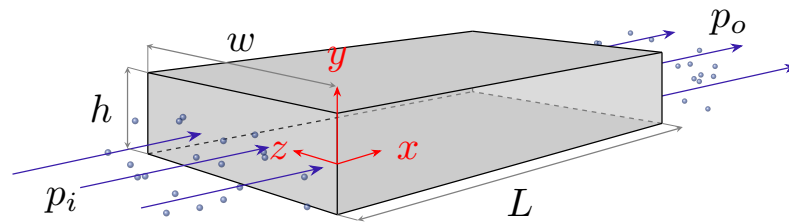


**Figure 1.** Schematic of pressure driven flow of a rarefied gas through a micro-channel of length  $L$ , height  $h$  and width  $w$  ( $L, w \gg h$ ).

Arkilic et al. [11] in his work on slip flows in micro-channels has categorised the flow regimes based on Mach number,  $Ma$ , and Reynolds number,  $Re = \rho u h / \mu$ . In this work we are interested in flow regimes with low Mach numbers,  $Ma \sim O(\epsilon)$  and low Reynolds number,  $Re \sim O(\epsilon)$ , i.e., the flows having Knudsen numbers of  $O(1)$ , given by the relation:

$$Kn = \sqrt{\frac{\pi}{2} \gamma} \frac{Ma}{Re}, \tag{5}$$

where  $\gamma$  is the specific heat ratio. In these flow regimes with  $Kn \sim O(1)$ , the wall-normal velocity and stream-wise gradients of  $u$  are insignificant as is evident by an order of magnitude analysis [11,25]. Therefore under the assumption of a steady-state fully developed flow, and neglecting the above terms and non-linear terms, the governing equations reduce to the following form:

$$\frac{\partial(\rho u)}{\partial x} = 0, \tag{6}$$

$$\frac{\partial}{\partial y} \left( \mu \frac{\partial u}{\partial y} \right) = \frac{\partial P}{\partial x}, \tag{7}$$

$$\frac{\partial P}{\partial y} = 0. \tag{8}$$

The reduced  $y$ -momentum equation, Equation (8), implies that pressure in the channel is a function of stream-wise coordinate, i.e.,  $P = P(x)$ , and from the reduced continuity and the  $x$ -momentum equation we can infer the stream-wise velocity,  $u$ , is a function of coordinates  $x$  and  $y$ .

### 2.2. Slip boundary Conditions

In most flow regimes where  $Kn$  is quite small ( $Kn \leq 0.001$ ), no slip boundary condition is used to describe velocity at the solid interface. The condition assumes that the velocity of the fluid layer in direct contact with the boundary is identical to the velocity of the boundary, i.e.,

$$u_{slip} = u - u_w = 0, \tag{9}$$

where  $u_w = 0$  is the velocity of the stationary solid wall. However, it is now well established that this condition fails to predict the near-wall velocity for rarefied gas flows. In 1879, Maxwell [22] introduced a first order slip formulation widely known as Maxwell slip, which is of the form:

$$u_{slip} = K_s \lambda \frac{\partial U_x}{\partial y} + \frac{3}{4} \frac{\mu}{\rho T} \frac{\partial T}{\partial x}, \tag{10}$$

where  $\lambda$  is the mean free path and  $K_s$  is the standard slip coefficient. The temperature gradient term in Equation (10) can be neglected under the current assumption of an isothermal flow but the term is important to predict flows arising from thermal gradients at the interface [31]. Researchers have also suggested a slip-velocity dependent on pressure gradients of the form [25,32]:

$$\rho u_{slip} \propto -\frac{\mu}{P} \frac{\partial P}{\partial x}. \tag{11}$$

The definition of slip velocity in Equation (11) is reminiscence of the diffusion component in the expression of volume-velocity in Recast Navier–Stokes system of equations [20,21]. Conventionally, derivation of continuum flow models as well as their analysis is routinely based on the flow’s mass-velocity (i.e., a velocity definition based on mass-averaging). Recast Navier–Stokes equations (RNS) developed in [20] define three type of volume-velocity variables,  $U_v$ ,  $U_T$  and  $U_p$ , that are each a sum of the standard mass-velocity,  $U_m$ , and a diffusion velocity component which takes into account one of the thermodynamic variable, namely, density, temperature or pressure, as:

$$U_v = U_m + \kappa_m \nabla \ln \rho = U_m + \frac{\kappa_m}{\rho} \nabla \rho, \tag{12}$$

where  $\kappa_m$  is a molecular diffusivity coefficient,

$$U_T = U_m + \kappa_T \nabla \ln T = U_m + \frac{\kappa_T}{T} \nabla T, \tag{13}$$

where  $\kappa_T$  is a molecular thermal diffusivity coefficient, and

$$U_p = U_m + \kappa_p \nabla \ln P = U_m + \frac{\kappa_p}{P} \nabla P, \tag{14}$$

where  $\kappa_p$  is a molecular pressure diffusivity coefficient. In a standard flow simulation a slip or no-slip boundary conditions may be adopted on the mass velocity,  $U_m$ . In this paper we propose to set these boundary conditions using the new velocity variables described in the RNS system. For example, in the pressure-driven flow in a micro- or nano-channel, we set a slip or no-slip on the pressure-diffusion velocity,  $U_p$ , defined in Equation (14). For a 2-dimensional rectangular channel as detailed in Figure 1, setting a first-order Maxwellian

slip boundary condition on the stream-wise volume-velocity  $u_p$  translates into the following mass-velocity boundary conditions:

$$u_{slip} = -\frac{\kappa_p}{P} \frac{\partial P}{\partial x} \mp K_s K_b \frac{\partial U_x}{\partial y} \quad \text{at } y = \pm \frac{h}{2}. \tag{15}$$

Here  $K_b = \lambda$  in the case of gas flow and  $K_s$  is the standard slip coefficient. Reddy and Dadzie [33] in their work on the effects of molecular diffusivity on shock-wave structures in monatomic gases assumed the following form for the molecular pressure diffusivity coefficient:

$$\kappa_p = \alpha_p \mu / \rho.$$

In the present paper, we consider the above relation for the molecular pressure-diffusivity coefficient where the coefficient  $\alpha_p$  is the phenomenological coefficient determined from the experimental data.

### 2.3. Effects of Rarefaction

Various length scales exist in the evaluation of gas micro-flows. At the molecular level, the mean free path (MFP) is considered along with other characteristic length scales such as mean molecular diameter and mean molecular spacing. In microfluidics where solid boundaries enclose the fluid, the MFP may be smaller than the characteristic length scale of the system and surface effects must be taken into account. The idea of “effective MFP”,  $\lambda_e$ , as a spatially varying function near the wall, can be traced back to the work of Stops [34]. Non-linear constitutive relations may be developed by incorporating effective-transport coefficients such as diffusivity, viscosity and thermal-conductivity based on  $\lambda_e$ , thereby accounting for rarefaction effects in a continuum description [35–38].

In the present work we adopt the definition of mean free path ( $\lambda$ ) provided by G.A. Bird [16]

$$\lambda = \frac{\mu}{P} \sqrt{\frac{\pi}{2} \mathcal{R}T}. \tag{16}$$

The associated Knudsen (Kn) number for the micro-channel shown in Figure 1, with a characteristic length  $h$ , pressure  $P$  and temperature  $T$  is:

$$\text{Kn} := \frac{\lambda}{h} = \frac{\mu}{hP} \sqrt{\frac{\pi}{2} \mathcal{R}T}. \tag{17}$$

Beskok and Karniadakis [35] in their rarefaction theory suggested a Bosanquet-type of expression for the viscosity in the transition regime and conducted numerical computations of flow in cylinders and channels using the Navier–Stokes equations complemented with slip boundary conditions. They suggested a Knudsen number dependent effective viscosity with a parameter  $a$ . Their formulation of the effective viscosity was of the form:

$$\mu_e := \mu \frac{\lambda_e}{\lambda} = \frac{\mu_0}{1 + a\text{Kn}}. \tag{18}$$

In the present study we adopt the above effective viscosity model in Equation (18) and assume  $a$  to be a constant as seen in the works of Michalis [38] and Lv [37]. Using this in our diffusion-slip model we incorporate the rarefaction effects into the molecular pressure diffusivity as:

$$\kappa_p := \alpha_p \frac{\mu_e}{\rho} = \frac{\alpha_p}{1 + a\text{Kn}} \cdot \frac{\mu_0}{\rho} \tag{19}$$

### 2.4. Analytical Solution

We solve the reduced governing equations Equations (6)–(8), along with the following boundary conditions,

$$u = \pm K_s K_b \frac{\partial u}{\partial y} - \frac{\kappa_p}{P} \frac{dP}{dx} \quad \text{at } y = \pm \frac{h}{2}, \tag{20}$$

$$P = P_{in} \quad \text{at } x = 0, \tag{21}$$

$$P = P_o \quad \text{at } x = L. \tag{22}$$

The velocity profile can be derived as a function of the pressure gradient by solving the  $x$ -momentum equation satisfying the boundary condition in Equation (20) as:

$$u = \frac{1}{2\mu} \frac{dP}{dx} \left( y^2 - \frac{h^2}{4} - \frac{2\mu\kappa_p}{P} - K_s K_b h \right). \tag{23}$$

Integrating this expression for the stream-wise velocity along the height of the channel and multiplying with the width,  $w$ , we get the expression for volumetric flux:

$$\dot{Q} = \int_{-\frac{h}{2}}^{\frac{h}{2}} w u dy, \tag{24}$$

$$= -\frac{wh^3}{12\mu} \frac{dP}{dx} \left( 1 + \frac{12\mu\kappa_p}{Ph^2} + \frac{6K_s}{h} K_b \right). \tag{25}$$

Mass flow rate through the micro-channel is calculated by integrating the density times volumetric flux across the length of the channel,

$$\dot{M} = \frac{1}{L} \int_0^L \rho \dot{Q} dx. \tag{26}$$

For the case of an incompressible fluid, the density of the fluid is constant, and we substitute the expression  $K_s K_b$  in the equation [see Equation (25)] with slip-length,  $K_l$ . This gives us

$$\begin{aligned} \dot{M} &= \frac{\rho}{L} \int_0^L \dot{Q} dx, \\ &= \frac{wh^3 \rho \Delta P}{12\mu L} \left( 1 + \frac{12\mu\kappa_p}{h^2 \Delta P} \ln \mathcal{P} + \frac{6K_l}{h} \right). \end{aligned} \tag{27}$$

Following the above procedure, the expression for mass flow rate of incompressible fluid through a cylindrical tube with radius 'R' and length 'L' can be derived in cylindrical coordinates as,

$$\begin{aligned} \dot{M} &= \frac{\pi R^4 \rho \Delta P}{8\mu L} \left( 1 + \frac{8\mu\kappa_p}{R^2 \Delta P} \ln \mathcal{P} + \frac{4K_l}{R} \right), \\ &= \dot{M}_{HP} \left( 1 + \frac{8\mu\kappa_p}{R^2 \Delta P} \ln \mathcal{P} + \frac{4K_l}{R} \right), \end{aligned} \tag{28}$$

where  $\dot{M}_{HP}$  is the mass flow rate relation predicted by the classical Haigen-Poiseuille law. Stamiatiou et al. [21] uses the RNS system of equations and no-slip condition at the wall to derive an equation for mass flow rate for liquid flow through micro-channel as:

$$\dot{M}_{RNS} = \frac{\pi R^4 \rho \Delta P}{8\mu L} \left( 1 + \frac{8\mu\kappa_p}{R^2 \Delta P} \ln \mathcal{P} \right). \tag{29}$$

It is evident that including effect of first order slip to the above relation gives us the mass flow rate expression derived with the present model, in Equation (28).

In the case of compressible fluid flowing through nano- and micro-channels, we consider expression for volumetric flow rate, Equation (25), where molecular diffusivity,  $\kappa_p$ , is substituted as per Equation (19). The rarefaction effects are included by replacing viscosity with an effective viscosity as given in Equation (18) and  $K_b = \lambda$  as  $\lambda_0\rho_0/\rho$ , respectively. We then substitute  $\rho$  with ideal gas equation, Equation (4) to get the expression of volumetric flux for the compressible case as,

$$\dot{Q} = -\frac{wh^3}{12\mu} \frac{dP}{dx} (1 + aKn) \left[ 1 + \frac{24\alpha_p}{\pi} \frac{Kn^2}{(1 + aKn)^2} + 6K_sKn \right], \tag{30}$$

where the Knudsen number, Kn is defined as per Equation (17). Under the assumption of isothermal flow we also have the following expression relating the pressure and Knudsen number at the outlet ( $P_o, Kn_o$ ) with pressure and Knudsen number inside the channel:

$$Kn_o P_o = Kn P. \tag{31}$$

We use the expression of volumetric flux for a compressible gas, Equation (30) and calculate the mass flow rate in the channel with Equation (26) as,

$$\dot{M} = \dot{M}_{NS} \left[ 1 + \frac{48\alpha_p}{\pi} \frac{Kn_o^2}{P^2 - 1} \ln\left(\frac{P + aKn_o}{1 + aKn_o}\right) + \frac{2K_sKn_o(a + 6K_s)}{P + 1} + \frac{12aK_sKn_o^2}{P^2 - 1} \ln P \right], \tag{32}$$

where  $\mathcal{P} = P_{in}/P_o$  is the ratio of pressures at the inlet and outlet of the channel and  $\dot{M}_{NS}$  is the mass flow rate expression for compressible flow through a pipe with no-slip boundary condition, and its expression is given by:

$$\dot{M}_{NS} = \frac{wh^3}{24\mu L RT} P_o^2 (\mathcal{P}^2 - 1).$$

To derive the expression for pressure profiles we utilise the fact that mass flux across any arbitrary cross-section of the channel is constant. i.e.,  $\dot{M}_A = \rho\dot{Q} = \text{constant}$ . Substituting the expression for  $\kappa_p$  and  $\dot{Q}$  from Equation (30) and rearranging the terms we get a differential equation in pressure of the form,

$$\frac{dP}{dx} \left( P + B + \frac{C}{P + D} + \frac{E}{P} \right) = -Z = \frac{F}{A}, \tag{33}$$

where  $A = wh^3/(12\mu\mathcal{R}T)$ ,  $B = (a + 6K_s)Kn_oP_o$ ,  $C = 24\alpha_p(Kn_oP_o)^2/\pi$ ,  $D = aKn_oP_o$ ,  $E = 6aK_s(Kn_oP_o)^2$  and  $F = \rho\dot{Q}$ .

Integrating the above differential equation for pressure with respect to  $x$ , we get a function in pressure:

$$f(P(x)) := \frac{P(x)^2}{2} + BP(x) + C \ln(P(x) + D) + E \ln P(x) = -Zx + C_1.$$

In the above expression  $Z = (f(P_{in}) - f(P_o))/L$  and the constant of integration,  $C_1 = f(P_{in})$  are calculated from the value of function  $f(P)$  at  $x = 0$  and at  $x = L$ . The pressure profiles as a function of the stream-wise coordinate,  $P(x)$ , can be calculated numerically by solving the equation,

$$f(P(x)) = f(P_{in}) - (f(P_{in}) - f(P_o)) \frac{x}{L}$$

By rearranging Equation (33) we get the following expression for pressure gradient along the stream-wise direction,

$$\frac{dP}{dx} = -\frac{1}{L} \frac{f(P_{in}) - f(P_o)}{P + B + \frac{C}{P+D} + \frac{E}{P}}. \tag{34}$$

The stream-wise velocity profile for the compressible fluid flow in the channel shown in Figure 1 can be written as a function of Knudsen number by rewriting Equation (23) to include effective viscosity and rarefaction effects:

$$u = \frac{1}{2} \frac{h^2}{\mu_e} \frac{dP}{dx} \left[ \left( \frac{y}{h} + \frac{1}{2} \right) \left( \frac{y}{h} - \frac{1}{2} \right) - \frac{4\alpha_p}{\pi} \frac{\text{Kn}^2}{(1 + a\text{Kn})^2} - K_s \text{Kn} \right]. \tag{35}$$

In the limit of  $\text{Kn} \rightarrow 0$ , the above velocity expression converges to the classical parabolic expression, but when  $\text{Kn} \gg O(1)$ , the diffusion and slip terms dominate in magnitude and the dependence of the stream-wise velocity on the wall-normal coordinate is reduced, thereby, attaining a plug-flow profile with corresponding slip at the walls,

$$u \approx \frac{1}{2} \frac{h^2}{\mu_e} \frac{dP}{dx} \left[ -\frac{4\alpha_p}{\pi} \frac{\text{Kn}^2}{(1 + a\text{Kn})^2} - K_s \text{Kn} \right]. \tag{36}$$

### 3. Results and Discussion

Using the expression for mass flow rate, Equation (32), derived in the previous section, we can predict the mass flow rates for helium gas in a long micro-channel for the various Knudsen regimes covered in the experiment of Ewart et al. [13], whose conditions are summarised in Table 1. The value for model parameter  $K_s = 1.1466$ , is chosen as per the first order slip coefficient reported by Cercignani [39] and Srekanth [40]. Phenomenological coefficients,  $\alpha_p = 0.3724$  and  $a = 0.4614$ , are determined by fitting with the experimental data of Ewart et al. [13].

In Figure 2 we compare the present results with the experimental data and previous studies as dimensionless flow rate,  $G$ , versus mean Knudsen number,  $\text{Kn}_m$ . The non-dimensional flow rate is defined as,

$$G = \dot{M} \left[ \frac{L\sqrt{2\mathcal{R}T}}{wh^2P_o(\mathcal{P} - 1)} \right],$$

and the mean Knudsen number,  $\text{Kn}_m$ , is calculated using Equation (17) at a mean pressure of  $(P_{in} + P_o)/2$ .

**Table 1.** Experimental conditions of Ewart et al. [13] for a pressure ratio of  $\mathcal{P} = 5$ .

Experimental Parameters	Value
Gas used	Helium
Length, $L$	$9.39 \pm 0.1$ mm
Height, $h$	$9.38 \pm 0.2$ $\mu\text{m}$
Width, $w$	$492 \pm 1$ $\mu\text{m}$
Avg. Temperature, $T$	296 K
Viscosity, $\mu$	$1.967 \times 10^{-5}$ Pa s
Gas Constant, $\mathcal{R}$	2078.5 J/(kg K)
Inlet Pressure range	60.4–109,825 Pa
Outlet Pressure range	12.2–22,633 Pa
Average Kn range	0.027–50.2

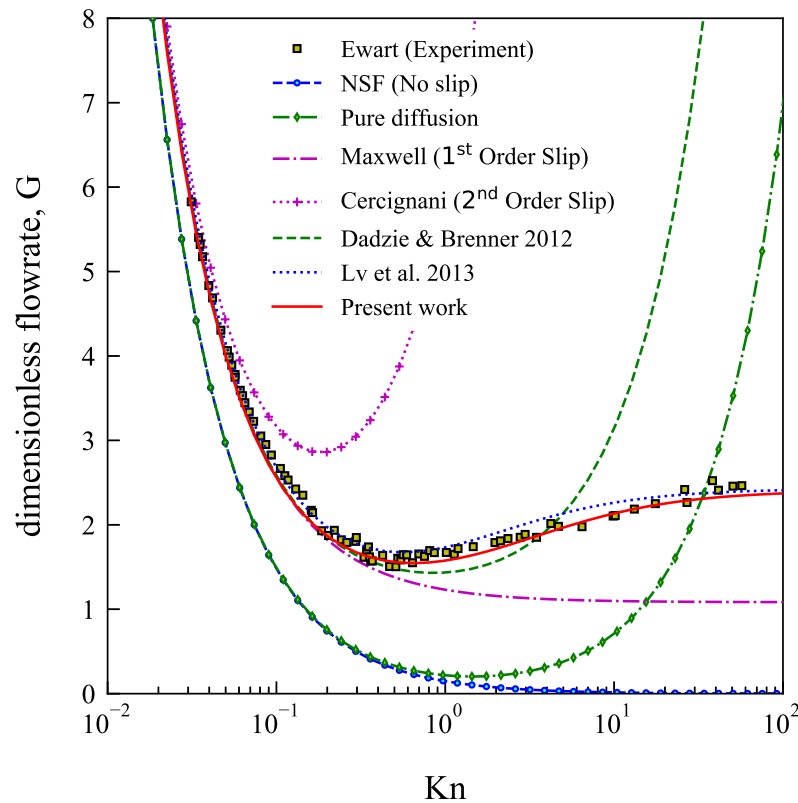


**Figure 2.** (Color Online) Comparison of dimensionless flow rate,  $G$ , versus the mean Knudsen number,  $Kn_m$ , between current work and other analytical expressions and the experimental data by Ewart et al. [13,30,37].

We observe in Figure 2 that the N-S solution with no-slip boundary conditions and pure diffusion boundary conditions diverge significantly from the experimental data, even in the slip flow regime ( $0.001 < Kn_m < 0.1$ ). The used of Maxwell's first order slip boundary conditions predicts the mass flow rate up to  $Kn_m < 0.5$ . Dadzie and Brenner [30] used a first order slip along with the bi-velocity continuum model as the governing equations to predict the mass flow rate. Their model is able to capture the Knudsen minimum and predicts the mass flow rate up to  $Kn_m = 5$  beyond which the model shows a diverging upward trend. The analytical formulation by Lv et al. [37] which also invokes a bi-velocity formulation shows significant improvement by addressing the rarefaction effects and captures the Knudsen minimum and mass flow rate trend in the whole  $Kn$  range. Our present model follows this, matching the experimental data well along the whole range of Knudsen number up to 50 with a better fit than Lv et al. model in the transition regime.

In Figure 3, a comparison is made of normalized stream-wise pressure distributions against the experimental data of Pong et al. [41] and analytical solution for pressure profile provided by Arkilic et al. [11] at various pressure ratios ( $\mathcal{P}$ ). Here, pressure is normalized with the outlet pressure of the micro-channel and the pressure ratio is defined as the ratio of inlet to outlet pressure. The measurements by Pong et al. [41] were made by embedding measurement ports in a micro-channel in which pressure transducers were mounted. The working gas was nitrogen and the outlet Knudsen number was fixed at 0.044. The current model predicts the non-linear pressure profiles very accurately within the errors of the experiment as seen in Figure 3.

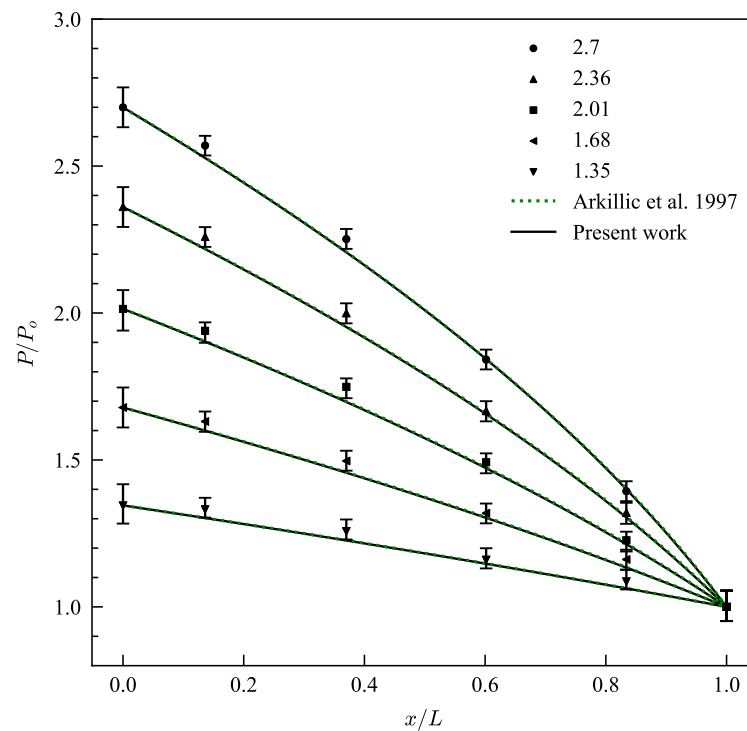


**Figure 3.** (Color Online) Pressure profiles along the micro-channel for various inlet-outlet pressure ratios as predicted by the current model (solid-line) plotted against the experimental data by Pong et al. [41] and pressure profiles predicted by analytical solution of Arkilic et al. [11].

The variation of non-linearity in the pressure distribution predicted by the current model can be better understood in the comparison made in Figure 4. In this figure the pressure non-linearity expressed as,  $(P - P_{lin}) / (P_{in} - P_o)$ , measures the deviation from a linear pressure profile from the incompressible flow case,  $P_{lin}$ . The comparison of pressure profiles are made for various outlet pressures with fixed pressure ratio of  $\mathcal{P} = 4$ . We have considered outlet pressures  $0.25P_{ch}$ ,  $0.5P_{ch}$ ,  $P_{ch}$ ,  $2P_{ch}$  and  $4P_{ch}$  which correspond to outlet Knudsen numbers of 4, 2, 1, 0.5 and 0.25, respectively, where  $P_{ch} = \frac{\mu}{h} \sqrt{\frac{\pi RT}{2}}$  is pressure at which outlet Knudsen number is 1. There is an apparent asymmetry observed in the pressure profiles in Figure 4. The location of the peaks or dips depend on the inlet/outlet pressure ratio and the Knudsen number. Current slip model predicts that with increase in Kn, the curvature of the nonlinear pressure distribution changes from a convex profile with respect to origin to a concave profile. The change in curvature of pressure profile is also captured by volume diffusion hydrodynamic model [42], second-order slip model [18] and ENSE with a diffusion boundary condition [32]; however, N-S equations with Maxwell's first-order slip model fails to predict this phenomena.

We use the analytical solution for the stream-wise velocity in Equation (35) to plot the velocity profiles for a micro-channel at various states of rarefaction. In Figure 5 we see that the current model predicts a parabolic profile with a small slip for  $Kn = 0.01$ . As the Knudsen number increases, slip increases until the parabolic profiles with slip at the wall becomes a full plug flow profile in the free molecular regime at  $Kn = 10$ . It is evident from Equation (35) that in the limit of  $Kn \rightarrow 0$ , the analytical solution for velocity converges to the description of a parabola as is the case in the continuum regime. The progression of the flow profile from a parabola with slip to a full plug flow is seen in the stream-wise velocity contours in Figure 6.

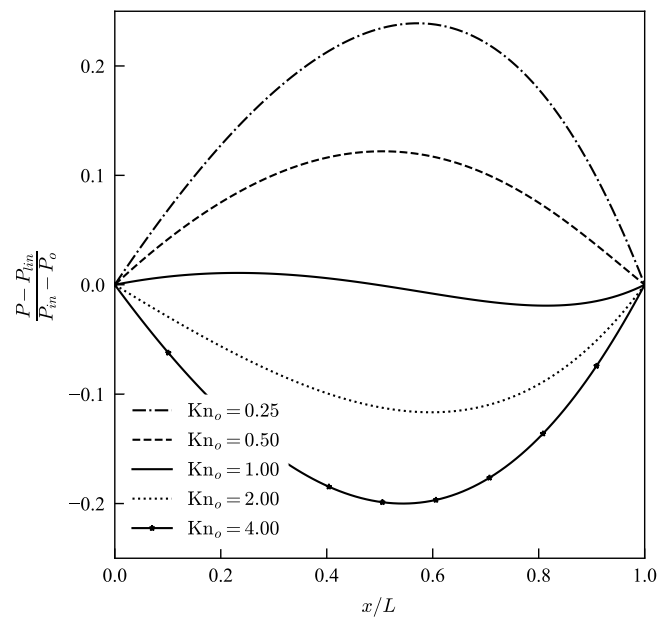


**Figure 4.** Variation in non-linearity of pressure profiles along the micro-channel for a pressure ratio  $\mathcal{P} = 4$ , plotted for various outlet pressure conditions.

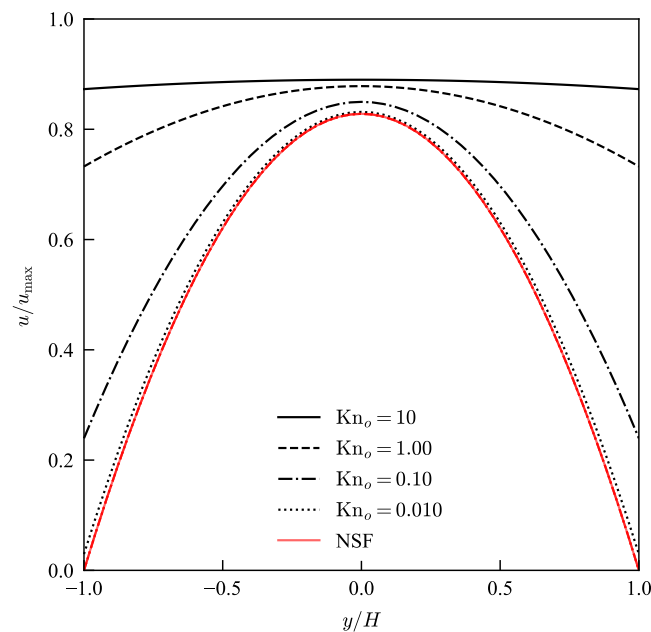


**Figure 5.** (Color Online) Comparison of normalised stream-wise velocity plotted as a function of normalised height,  $y/H$ , at location  $X = 0.9$  along the micro-channel, for various Knudsen numbers as predicted by current model (in black) and N-S with no-slip condition (in red). The velocity profiles are normalised with the corresponding maximum value for each case which corresponds to the exit velocity along the center-line of the pipe.

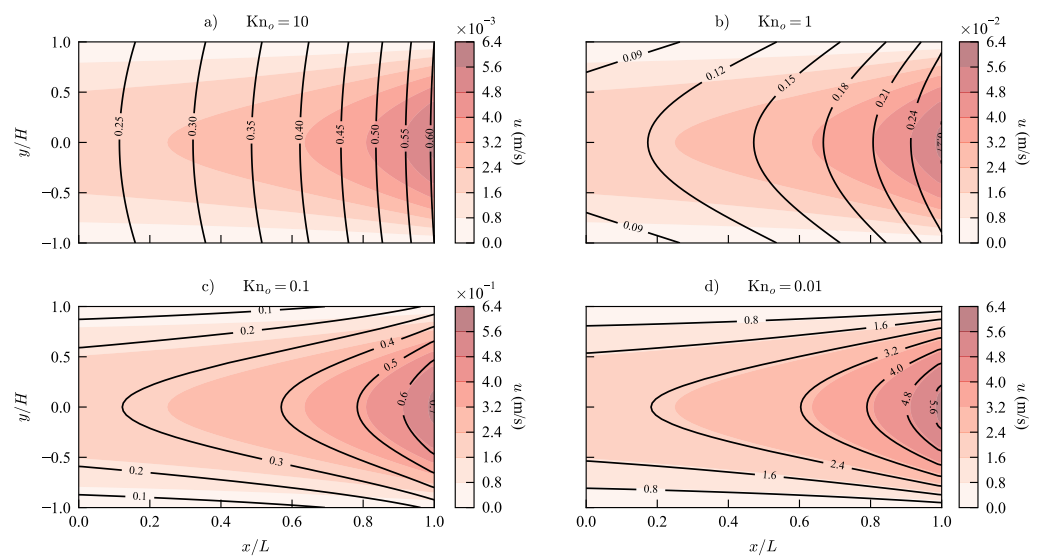


**Figure 6.** (Color Online) Stream-wise velocity contours predicted by the new model for outlet pressure conditions corresponding to Knudsen numbers (a) 10, (b) 1, (c) 0.1 and (d) 0.01. The velocity contour lines are plotted over the stream-wise velocity contour field for a typical parabolic velocity profile predicted by N-S equations with no slip boundary condition.

#### 4. Conclusions

In this article, we developed a diffusion-slip model that predicts mass flow rates, velocity distribution and pressure profiles in a rectangular channel over the entire flow regime. The new slip model is a three-parameter model and is able to predict the Knudsen minimum that occurs in the transitional regime. The model compares well against other analytical solutions in predicting the mass flow rates up to free molecular regime.

The proposed diffusion-slip model derived from adopting the definition of other type of velocity variables alongside the conventional mass velocity as seen in the recast Navier–Stokes models [20]. Setting a first order Maxwell’s slip boundary conditions on the new velocity variable leads to the new diffusion-slip model. This investigation strengthens the usefulness of the concept of volume diffusion and the definitions of the new velocity variables. The article also details on the variation of pressure profiles for micro-channels with rarefaction. The present model is able to capture the non-linearity and the change in curvature of pressure profiles with increasing Knudsen number as reported in the literature. A characteristic pressure is determined below which the flow is dominated by diffusion. The velocity profiles predicted by using the new slip model with N-S equations agree with the trends observed in a micro-channel at various states of rarefaction. In the free molecular regime, the diffusive terms have a larger effect in governing the flow profiles, thereby giving a plug flow velocity profile along the channel. This plug flow profile can be noted in the numerical simulations in the works of Christou and Dadzie [43]. The new slip conditions and analytical solutions provide an alternative physical explanation for rarefied flows in micro-channels and may be adopted to interpret other non-equilibrium flow phenomena.

**Author Contributions:** Conceptualization and methodology proposed by S.K.D. Analytical development and numerical implementation and editing by A.M.T. All authors have read and agreed to the published version of the manuscript.

**Funding:** This research was funded by the Leverhulme Trust, UK, under Research Project Grant: RPG-2018-174.

**Conflicts of Interest:** The authors declare no conflict of interest.

## References

1. Karniadakis, G.; Beskok, A.; Aluru, N. *Microflows and Nanoflows: Fundamentals and Simulation*; Springer: New York, NY, USA, 2006; Volume 29. [[CrossRef](#)]
2. Whitesides, G.M. The origins and the future of microfluidics. *Nature* **2006**, *442*, 368–373. [[CrossRef](#)] [[PubMed](#)]
3. Stone, H.A.; Stroock, A.D.; Ajdari, A. Engineering flows in small devices: Microfluidics toward a lab-on-a-chip. *Annu. Rev. Fluid Mech.* **2004**, *36*, 381–411. [[CrossRef](#)]
4. Gad-el Hak, M. The Fluid Mechanics of Microdevices—The Freeman Scholar Lecture. *J. Fluids Eng.* **1999**, *121*, 5–33. [[CrossRef](#)]
5. Wei, T. All-in-one design integrates microfluidic cooling into electronic chips. *Nature* **2020**, *585*, 188–189. [[CrossRef](#)] [[PubMed](#)]
6. Brenner, H. Beyond Navier–Stokes. *Int. J. Eng. Sci.* **2012**, *54*, 67–98. [[CrossRef](#)]
7. Majumder, M.; Chopra, N.; Andrews, R.; Hinds, B.J. Enhanced flow in carbon nanotubes. *Nature* **2005**, *438*, 44. [[CrossRef](#)]
8. Whitby, M.; Quirke, N. Fluid flow in carbon nanotubes and nanopipes. *Nat. Nanotechnol.* **2007**, *2*, 87. [[CrossRef](#)]
9. Hemadri, V.; Varade, V.V.; Agrawal, A.; Bhandarkar, U. Investigation of rarefied gas flow in microchannels of non-uniform cross section. *Phys. Fluids* **2016**, *28*, 022007. [[CrossRef](#)]
10. Knudsen, M. Die Gesetze der Molekularströmung und der inneren Reibungsströmung der Gase durch Röhren. *Ann. Phys.* **1909**, *333*, 75–130. [[CrossRef](#)]
11. Arkilic, E.B.; Schmidt, M.A.; Breuer, K.S. Gaseous slip flow in long microchannels. *J. Microelectromech. Syst.* **1997**, *6*, 167–178. [[CrossRef](#)]
12. Maurer, J.; Tabeling, P.; Joseph, P.; Willaime, H. Second-order slip laws in microchannels for helium and nitrogen. *Phys. Fluids* **2003**, *15*, 2613–2621. [[CrossRef](#)]
13. Ewart, T.; Perrier, P.; Graur, I.A.; Méolans, J.G. Mass flow rate measurements in a microchannel, from hydrodynamic to near free molecular regimes. *J. Fluid Mech.* **2007**, *584*, 337–356. [[CrossRef](#)]
14. Cheng, J.T.; Giordano, N. Fluid flow through nanometer-scale channels. *Phys. Rev. E* **2002**, *65*, 031206. [[CrossRef](#)]
15. Kavokine, N.; Bocquet, M.L.; Bocquet, L. Fluctuation-induced quantum friction in nanoscale water flows. *Nature* **2022**, *602*, 84–90. [[CrossRef](#)] [[PubMed](#)]
16. Bird, G.A. *Molecular Gas Dynamics and the Direct Simulation of Gas Flows*; Oxford Engineering Science Series; Clarendon Press: Oxford, UK, 1994.
17. Chakraborty, S.; Durst, F. Derivations of extended Navier–Stokes equations from upscaled molecular transport considerations for compressible ideal gas flows: Towards extended constitutive forms. *Phys. Fluids* **2007**, *19*, 088104. [[CrossRef](#)]
18. Dongari, N.; Agrawal, A.; Agrawal, A. Analytical solution of gaseous slip flow in long microchannels. *Int. J. Heat Mass Transf.* **2007**, *50*, 3411–3421. [[CrossRef](#)]
19. Brenner, H. Bi-velocity hydrodynamics. *Physica A* **2009**, *388*, 3391–3398. [[CrossRef](#)]
20. Reddy, M.H.L.; Dadzie, S.K.; Ocone, R.; Borg, M.K.; Reese, J.M. Recasting Navier–Stokes equations. *J. Phys. Commun.* **2019**, *3*, 105009. [[CrossRef](#)]
21. Stamatiou, A.; Dadzie, S.K.; Reddy, M.L. Investigating enhanced mass flow rates in pressure-driven liquid flows in nanotubes. *J. Phys. Commun.* **2019**, *3*, 125012. [[CrossRef](#)]
22. Maxwell, J.C. VII. On stresses in rarified gases arising from inequalities of temperature. *Philos. Trans. R. Soc. Lond.* **1879**, *170*, 231–256. [[CrossRef](#)]
23. Duan, Z. Second-order gaseous slip flow models in long circular and noncircular microchannels and nanochannels. *Microfluid Nanofluid* **2012**, *12*, 805–820. [[CrossRef](#)]
24. Hemadri, V.; Agrawal, A.; Bhandarkar, U. Determination of tangential momentum accommodation coefficient and slip coefficients for rarefied gas flow in a microchannel. *Sādhanā* **2018**, *43*, 1–7. [[CrossRef](#)]
25. Adachi, T.; Sambasivam, R.; Durst, F.; Filimonov, D. Analytical treatments of micro-channel and micro-capillary flows. In Proceedings of the 3rd Micro and Nano Flows Conference, Thessaloniki, Greece, 22–24 August 2011; Brunel University: Thessaloniki, Greece, 2011; pp. 22–24.
26. Veltzke, T.; Thöming, J. An analytically predictive model for moderately rarefied gas flow. *J. Fluid Mech.* **2012**, *698*, 406–422. [[CrossRef](#)]
27. Dongari, N.; Durst, F.; Chakraborty, S. Predicting microscale gas flows and rarefaction effects through extended Navier–Stokes–Fourier equations from phoretic transport considerations. *Microfluid Nanofluid* **2010**, *9*, 831–846. [[CrossRef](#)]
28. Brenner, H. Navier–Stokes revisited. *Phys. Fluids* **2005**, *349*, 60–132. [[CrossRef](#)]
29. Brenner, H. Diffuse volume transport in fluids. *Physica A* **2010**, *389*, 4026–4045. [[CrossRef](#)]
30. Dadzie, S.K.; Brenner, H. Predicting enhanced mass flow rates in gas microchannels using nonkinetic models. *Phys. Rev. E* **2012**, *86*, 036318. [[CrossRef](#)]
31. Lockerby, D.A.; Reese, J.M.; Emerson, D.R.; Barber, R.W. Velocity boundary condition at solid walls in rarefied gas calculations. *Phys. Rev. E* **2004**, *70*, 017303. [[CrossRef](#)]
32. Jaishankar, A.; McKinley, G.H. An analytical solution to the extended Navier–Stokes equations using the Lambert W function. *AIChE J.* **2014**, *60*, 1413–1423. [[CrossRef](#)]
33. Reddy, L.M.H.; Dadzie, S.K. Effects of molecular diffusivity on shock-wave structures in monatomic gases. *Phys. Rev. E* **2021**, *104*, 035111. [[CrossRef](#)]
34. Stops, D. The mean free path of gas molecules in the transition regime. *J. Phys. D* **1970**, *3*, 685. [[CrossRef](#)]

35. Beskok, A.; Karniadakis, G.E. Report: A model for flows in channels, pipes, and ducts at micro and nano scales. *Microscale Thermophys. Eng.* **1999**, *3*, 43–77. [[CrossRef](#)]
36. Lockerby, D.A.; Reese, J.M.; Gallis, M.A. Capturing the Knudsen layer in continuum-fluid models of non-equilibrium gas flows. *AIAA J.* **2005**, *43*, 1391–1393. [[CrossRef](#)]
37. Lv, Q.; Liu, X.; Wang, E.; Wang, S. Analytical solution to predicting gaseous mass flow rates of microchannels in a wide range of Knudsen numbers. *Phys. Rev. E* **2013**, *88*, 013007. [[CrossRef](#)]
38. Michalis, V.K.; Kalarakis, A.N.; Skouras, E.D.; Burganos, V.N. Rarefaction effects on gas viscosity in the Knudsen transition regime. *Microfluid Nanofluid* **2010**, *9*, 847–853. [[CrossRef](#)]
39. Cercignani, C. *Mathematical Methods in Kinetic Theory*; Springer: New York, NY, USA, 1969. [[CrossRef](#)]
40. Sreekanth, A.K. Slip flow through long circular tubes. In Proceedings of the Sixth International Symposium on Rarefied Gas Dynamics, Cambridge, MA, USA, 22–26 July 1969; Academic Press: New York, NY, USA, 1969; pp. 667–680.
41. Pong, K.C.; Ho, C.M.; Liu, J.; Tai, Y.C. Non-linear pressure distribution in uniform microchannels. *Am. Soc. Mech. Eng.* **1994**, *197*, 51.
42. Dadzie, S.K.; Dongari, N. Transition regime analytical solution to gas mass flow rate in a rectangular micro channel. *AIP Conf. Proc.* **2012**, *1501*, 720–726. [[CrossRef](#)]
43. Christou, C.; Dadzie, S.K. On the numerical simulation of rarefied gas flows in micro-channels. *J. Phys. Commun.* **2018**, *2*, 035002. [[CrossRef](#)]